AGU ADVANCING EARTH AND SPACE SCIENCE

Water Resources Research

RESEARCH ARTICLE
10.1029/2022WR033878

Lysimeter and In Situ Field Experiments to Study Soil Evaporation Through a Dry Soil Layer Under Semi-Arid Climate

E. Balugani[1,2], M. W. Lubczynski[1], and K. Metselaar[3]

[1]Faculty of Geoinformation Science and Earth Observation ITC, University of Twente, Enschede, The Netherlands, [2]University of Bologna, Bologna, Italy, [3]Wageningen University, Wageningen, The Netherlands

Key Points:

- Development of an original lysimeter setup allowing for separate measurements of evaporation (E) and groundwater evaporation (E_g)
- Under dry soil layer condition, lysimeter $E = E_g$, ~1.25 mm days^{-1} in 2012 and 1.05 mm days^{-1} in 2015
- Lysimeter evaporation correlated with profile soil temperature measurements and solar radiation changes; vapor diffusion was negligible

Supporting Information:

Supporting Information may be found in the online version of this article.

Correspondence to:

E. Balugani and M. W. Lubczynski, enricobalugani82@gmail.com; m.w.lubczynski@utwente.nl

Citation:

Balugani, E., Lubczynski, M. W., & Metselaar, K. (2023). Lysimeter and in situ field experiments to study soil evaporation through a dry soil layer under semi-arid climate. *Water Resources Research*, *59*, e2022WR033878. https://doi.org/10.1029/2022WR033878

Received 12 OCT 2022
Accepted 20 JAN 2023

Author Contributions:

Conceptualization: E. Balugani, K. Metselaar
Data curation: E. Balugani
Formal analysis: K. Metselaar
Funding acquisition: M. W. Lubczynski
Investigation: E. Balugani
Methodology: E. Balugani, M. W. Lubczynski
Project Administration: M. W. Lubczynski
Resources: E. Balugani, M. W. Lubczynski
Software: E. Balugani

Abstract During droughts, soil evaporation is often constrained by water vapor transport through an air-dry soil layer (DSL). Fick's water vapor diffusion is widely regarded as the only process for such transport; however, field studies conducted in arid and semi-arid conditions showed measured evaporation rates higher than those predicted by diffusion. Therefore, transport processes other than diffusion could be relevant. To study the evaporation through a DSL, the same lysimeter column with 70 cm thick DSL as earlier applied in laboratory in Balugani et al. (2021), was installed in the field in Spain applying an original weighing setup to measure evaporation. The correlation between the measured evaporation and possible drivers of the water vapor transport were evaluated. With the DSL thickness of 70 cm in 2012 and 12 cm in 2015, the lysimeter recorded similar groundwater evaporation rates: 1.25 and 1.05 mm days^{-1}, respectively; these rates were much larger than the laboratory recorded rates (0.3 mm days^{-1}) and those estimated in this study using Hydrus1D accounting for non-isothermal liquid water fluxes and water vapor diffusion. The main forcing driver of the field lysimeter evaporation was the soil profile temperature fluctuation, which concealed other less important forcing factors, that is, atmospheric pressure fluctuations and diffusion. A multivariate regression model to estimate evaporation was proposed, based on the profile temperature fluctuation, that, when added to the atmospheric pressure fluctuations, yielded reliable estimates of the cumulative evaporation measured in both 2012 and 2015.

1. Introduction

Soil evaporation in dry conditions is a complex process that is difficult to quantify (Brutsaert, 2014a, 2014b; Vanderborght et al., 2017). Dry environmental conditions happen any time, when there is a prolonged period without precipitation, resulting in soil moisture being progressively depleted by plant transpiration and soil evaporation. Droughts or dry spells occur in every climate during specific periods of a year (dry season), but are the norm in arid and semi-arid areas, which are often referred as water limited environments (Parsons & Abrahams, 1994). Long-term droughts happen also in other climates (subtropical, Mediterranean) and their frequency is increasing due to climate change (Mukherjee et al., 2018; Schlaepfer et al., 2017; Xu et al., 2019). They deplete water resources, but also negatively affect agricultural productivity. Therefore, understanding of evaporation processes and their quantification in dry conditions is especially important for water management and agriculture practices.

A characteristic feature of prolonged dry conditions is the formation of a dry soil layer (DSL, Figure 1), in which water is transported as vapor to the soil surface (Balugani et al., 2017; Brutsaert, 2014a, 2014b; Or et al., 2013). The formation of a DSL is due to the drying of a bare soil from the surface downward, or by the transpiration of grasses, typically at the start of the dry period; grass could then wither and be eliminated by fire, wind, grazing animals, or by humans, leaving behind a bare soil with a DSL. Thus, the formation of bare soil with DSL can occur on bare soil, pasture, or in the open soil areas between trees in open woodlands.

A schematization of the shallow water table evaporation process during a drought for a bare soil, is presented in Figure 1; under these conditions, total evaporation (E) is assumed equal to groundwater evaporation (E_g). At the beginning of a drought, when DSL is not yet present, the E_g process starts from the saturated zone, that is, from the drying front (Lehmann et al., 2008; Shokri & Or, 2011), above which the transport of water first takes place as upward liquid flow through the capillary zone, driven by capillary pressure and evaporated at the vaporization plane, which at that stage, is at the ground surface. With the ongoing evaporation process, the drying front moves downward and the liquid phase distribution above the receding drying front can be approximated by hydrostatic

Supervision: M. W. Lubczynski, K. Metselaar
Validation: E. Balugani
Visualization: E. Balugani
Writing – original draft: E. Balugani
Writing – review & editing: M. W. Lubczynski, K. Metselaar

saturation distribution such as above a water table where the medium remains saturated to a height equal to the capillary fringe (Shokri et al., 2008). When the drying front reaches a certain depth, equal to a critical length (L_c), at which capillary forces are too small to sustain hydraulic continuity, a layer with no hydraulic connection with the soil surface, that is, the DSL, develops. In the DSL, water in the vapor form, moves upward from the top of the capillary-driven zone called "vaporization plane" (Or et al., 2013) to the ground surface. Continuation of the evaporation process, results in the movement of the vaporization plane downward in the soil profile, leaving behind a DSL.

The formation of DSLs in bare soils has been observed in laboratory and field conditions. Laboratory experiments usually considered small soil columns (10–30 cm long, a few centimeters in diameter), initially saturated conditions, and stable evaporative conditions (Lehmann et al., 2008; Lehmann & Or, 2009; Or et al., 2013; Shokri & Salvucci, 2011). Few field lysimeter experiments considered long columns (1–2 m long, ∼1 m in diameter), initial conditions depending on the weather (with soil surface that may be covered by grass), and evaporation conditions determined by the weather (Assouline et al., 2013; Dijkema et al., 2017; Ma et al., 2019). The DSL thickness (Z_{DSL}) observed in laboratory conditions were in the order of ∼3–14 mm (Or et al., 2013), while in field conditions, ∼5–50 cm (Balugani et al., 2018; Wang, 2015).

Whereas it seems accepted that water is transported through the DSL as vapor, the main transport mechanism through the DSL is not clear yet (Brutsaert, 2014a, 2014b; Vanderborght et al., 2017), as different studies suggest different governing processes. Laboratory experiments conducted on small soil columns (Or et al., 2013) suggest that the water vapor transport in the DSL can be explained by Fick diffusion only (from hereafter referred as diffusion). As such, most hydrological soil models, for example, Hydrus1D (Simunek et al., 2008), implement diffusion as the only transport process of vapor in the DSL. Lysimeter experiments, however, often measure evaporation rates larger than those predicted by independently parameterized diffusion, when a DSL is present; this has been attributed to the temporally varying environmental conditions mainly affecting advective water fluxes, for example, due to: wind speed (Davarzani et al., 2014; Farrell et al., 1966; Fetzer et al., 2017; Scotter & Raats, 1969), thermal gradients (Saito et al., 2006; Zeng et al., 2007), daily cycles of condensation and evaporation of soil moisture at the vaporization plane, changing Z_{DSL} (Assouline et al., 2013; Deol et al., 2014), the effect of atmospheric pressure fluctuations (Balugani et al., 2021), the controversial enhanced vapor transport mechanism (Philip & de Vries, 1957; Webb & Ho, 1998), heterogeneous soil conditions leading to preferential evaporative fluxes (Or et al., 2013; Vanderborght et al., 2014), and natural convection in sloping dry soils (Rose & Guo, 1995). Since consensus has not been reached yet, in practice-oriented applications, the effect of the DSL on the evaporation process is often either neglected or parameterized as a "resistance term" (Vanderborght et al., 2017), with the underlying assumption that the forcing factors for evaporation are the same with or without a DSL.

The two main limitations to understanding the forcing factors of evaporation in a soil with a DSL are due to: (a) a mismatch between the conditions studied in the laboratory and in the field; and (b) the large amount of possible forcing factors in the field conditions. In order to address the (a) limitation, Balugani et al. (2021) devised a laboratory controlled lysimeter experiment, intending to repeat the same lysimeter setup in the field (the latter, presented hereafter). The laboratory experiment used large lysimeters (1 and 2 m long, ∼30 cm diameter) to determine the relevance of possible evaporative transport processes through a DSL with a thickness $Z_{DSL} > 50$ cm. In that experiment, Balugani et al. (2021) found that the evaporation by vapor flow through DSL was substantially larger than predicted by diffusion alone and that the main driving force of that process was atmospheric pressure fluctuation. In order to address limitation (b), the methodology of this study follows CO_2 soil flux studies, where the relevance of different gas phase transport processes is evaluated using the correlation between the measured CO_2 soil flux and the measured environmental forcing factors (Bowling et al., 2015; Roland et al., 2015; Sánchez-Cañete et al., 2013). To our knowledge, such an approach has not been used in soil DSL evaporation studies yet.

In this study, the laboratory lysimeter experimental setup used in Balugani et al. (2021) was replicated and tested in a semi-arid field study area, to measure vapor flow soil DSL evaporation. Then, the correlations of environmental forcing factors with the observed evaporation rates were analyzed applying a method based on CO_2 soil flux studies. Additionally, a nearby soil profile was also monitored to compare the lysimeter

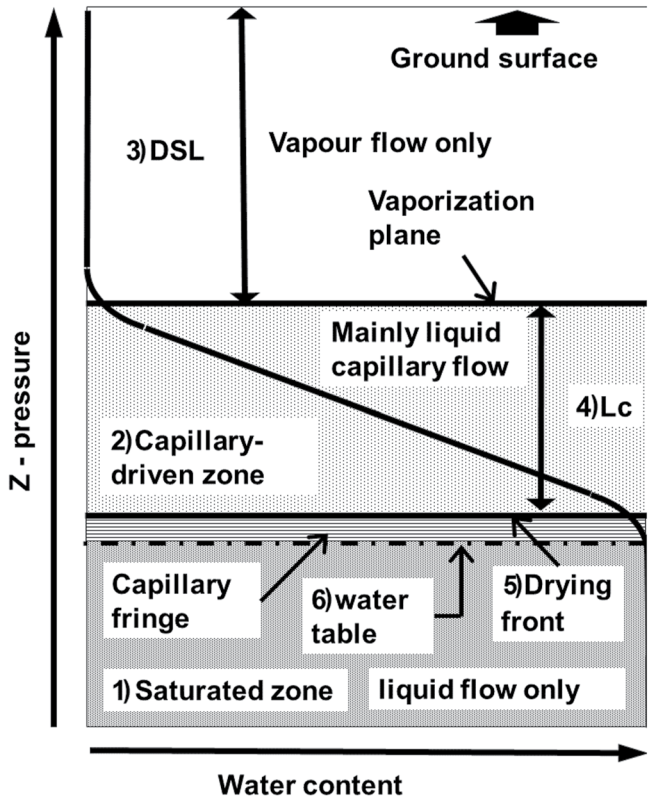

Figure 1. Schematics of a soil with a dry soil layer (DSL) as observed in laboratory experiments with a shallow water table under hydrostatic conditions (modified after Shokri & Salvucci, 2011). The meaning of numerators is as follow: 1) saturated zone; 2) capillary driven zone; 3) DSL; 4) critical length (L_c) at which capillary forces become too small to sustain hydraulic continuity (Or et al., 2013); 5) drying front; 6) water table level.

conditions with the actual soil conditions at the site. The scientific questions this study aimed to address were as follows:

- Is it possible to measure evaporation rates through a thick DSL, using the laboratory-tested lysimeter setup in the field conditions?
- Which forcing factors of vapor transport are able to explain the observed evaporation in a soil with a DSL in field conditions?
- How does an evaporation model derived using the forcing factors identified in this study, compare with an evaporation model that assumes liquid water flow and water vapor diffusion as the most relevant forcing factors, for example, the Hydrus1D model?

2. Materials and Methods

2.1. Field Measurements

The lysimeter experiment (2012–2015) was setup in the Trabadillo site in the Sardon Catchment, Spain (Figure 2a; latitude: 41.1172°, longitude: −6.1471°), an area characterized by semi-arid climate and already well equipped and studied by the authors (Balugani et al., 2017, 2018; Daoud et al., 2022; Francés et al., 2015; Hassan et al., 2014; Lubczynski & Gurwin, 2005; Reyes-Acosta & Lubczynski, 2014). Grass covers the soil only approximately 3 months a year in spring, then, during the dry season (starting in May-June), becomes dormant and is grazed by animals, leaving the soil bare. The mean yearly precipitation is ~600 mm yr^{-1}, with driest and wettest years ~300 and ~900 mm yr^{-1} respectively (Daoud et al., 2022). Most of the rain events are concentrated in spring (March–May) and fall (October–December), with no or very little rain in the period between mid-May and September (dry season). Winters are cold and humid, with relative humidity (RH) often at 100%, mean air temperature (T_a) ~5°C, frequent but mild precipitation (P < 100 mm $month^{-1}$) and average wind speed (u) ~2 m s^{-1}. The summers are warm and dry, with RH decreasing to 20% during a day, a mean T_a ~20°C, rare rainfall showers (P < 20 mm $month^{-1}$), maximum net short wave radiation S_n ~ 75 Mj m^{-2} $days^{-1}$, and u ~1.5 m s^{-1}.

The lysimeter was installed in the field (Figure 2a) in May 2012 with the same setup as the earlier laboratory experiment by Balugani et al. (2021). The field lysimeter consisted of a PVC column of 1 m height and a diameter of 0.28 m, wrapped in glass wool to insulate its walls from heat loss and connected with a 2 L Mariotte bottle at

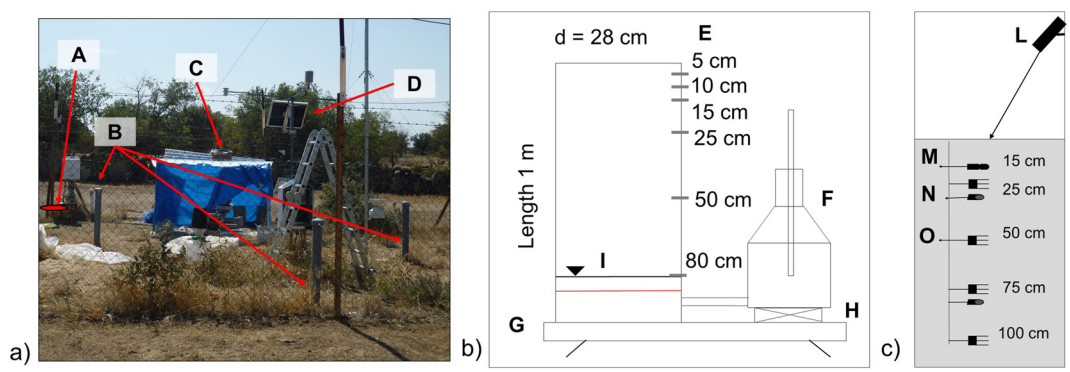

Figure 2. Monitoring setup: (a) Trabadillo study site (A - in situ soil monitoring profile; B - piezometers; C - lysimeter; D - weather station); (b) schema of the lysimeter column (E - depth markers of matric potential and temperature sensors; F - Mariotte bottle; G - lysimeter weighing device; H - Mariotte bottle weighing device; I - water table inside the column); (c) schema of the in situ soil monitoring profile (L - infrared radiometer; M - POT matric potential sensor; N - MPS1 matric potential sensor; and O - HydraProbe soil moisture and temperature sensor).

the bottom, to keep a fixed water table depth at 80 cm below the top of the lysimeter column. The Mariotte bottle was positioned at the top of the lysimeter base, so that the lysimeter weight included the weight of the Mariotte bottle. The lysimeter was filled to the top of the column, with the same material as in the earlier laboratory experiment, that is, well-sorted, oven-dried sand of 0.10–0.25 mm particle size, added with 1 cm layers at a time and carefully packed to avoid introducing heterogeneity in the porous medium. The final porosity of the sand was 0.40. The lysimeter was closed at the bottom and open at the top to allow evaporation but closed at the bottom.

The lysimeter was equipped with six matric potential ($\Psi_{L,\text{depth}}$) and temperature ($T_{L,\text{depth}}$) MPS1 sensors (Decagon, USA) installed as shown in Figure 2b. The weight of the Mariotte bottle, representing the amount of water entering or leaving the lower boundary of the soil column, was measured every 5 min, using a load cell (SM100, Interface, USA) installed in a device with accuracy 0.01 g (10^{-4} mm of water evaporated in the column). The accuracy of the lysimeter (∼300 kg), designed and constructed at the laboratory of the University of Twente (The Netherlands), was 30 g, corresponding to 0.03 L of water, or ∼0.5 mm of the lysimeter column.

The connection between the Mariotte bottle and the column bottom was tested by keeping it closed for 3 days to ensure the lack of leakages, then it was opened on 7 May 2012 while keeping the column top closed, allowing the water table to rise and stabilize at 20 cm above the column bottom, until the water flow from the Mariotte bottle to the dry soil column stopped. Then, on 13 May 2012, the lysimeter was left to equilibrate with atmospheric conditions for 9 days; during these 9 days the system was also checked for possible leakages. The fully automatized and protected experiment started on 22 May 2012 and was left in the field unattended (but monitored from the Netherlands); the data was collected on 10 September 2012 and it was found that the 2 L Mariotte bottle drained after only 19 days of experiment, much faster than expected.

The Mariotte bottle was not filled again with water in order to observe the natural replenishment from precipitation and then study the natural formation of a DSL under field evaporative conditions. So, the Mariotte bottle remained empty until the first rains in October 2012, when the precipitation events infiltrated in the lysimeter column and refilled the Mariotte bottle. In the dry July 2015 during lysimeter maintenance, the column was still saturated up to 78 cm above the column bottom (i.e., 22 cm depth below the column top), with the Mariotte bottle completely filled with water due to flooding of the column in the previous, medium-wet years 2013 and 2014 when DSL was not developed. During the maintenance in July 2015, the first 22 cm of the column soil, down to the water table, were removed for cleaning, which also allowed the observation of a 12 cm thick DSL, and a 10 cm L_c. Afterward, the soil material was placed back in the column, exactly as positioned before, and the experiment was continued. The amount of water in the column was not affected by the maintenance, hence the column was still saturated up to 78 cm when the experiment was started again. The lysimeter experiment was terminated in September 2015.

When the water table height (78 cm) in the column was higher than the water table height fixed in the Mariotte bottle at 20 cm depth above the lysimeter bottom, the Mariotte bottle could not be used to record E_g because the Mariotte bottle remained full of water. Therefore, the only measurements of evaporation (E) available after 2012 were those from the total lysimeter weight. The comparison between 2012 Mariotte bottle weight and 2015 lysimeter weight measurements, however, was still possible, since both weight measurements were done during dry periods, when DSLs were developed as in Figure 1 ($E \approx E_g$). The small water input from the rare rain events did not infiltrate more than few centimeters (no increase in the matric potential at 5 cm depth) and evaporated quickly, with negligible effects on the lysimeter weight.

The in situ soil in the study area is spatially homogeneous, with a texture between sandy-loam and loamy-sand, similar to the sand filling the lysimeter, but less well-sorted (Francés et al., 2014). The in situ soil monitoring profile was equipped with four soil moisture and temperature sensors (HydraProbe, Stevens, USA, at 25, 50, 75, and 100 cm b.g.s.), two matric potential sensors (Decagon MPS1 sensors at 25 and 75 cm b.g.s.) and another, more accurate matric potential sensor (POT, Bakker et al., 2007; range 0–1.5 MPa, at 15 cm b.g.s.), with a sampling time of 30 min. The MPS1 devices in the in situ soil profile and in the lysimeter, did not work properly between May 2012 and June 2013.

The following depth-dependent variables were measured: soil moisture ($\theta_{s,\text{depth}}$), soil temperature ($T_{s,\text{depth}}$) and matric potential ($\Psi_{s,\text{depth}}$). Besides, a temperature radiometer measured the temperature of the soil surface every 5 min (same value for both lysimeter and in situ soil, T_0). The weather station provided also hourly data of relative humidity (RH), air temperature (T_a), net short-wave radiation (S_n), wind speed (u), atmospheric pressure (p_{atm}), rainfall (P), and water table depth (Z_{WT}) from a nearby piezometer.

2.2. Analysis of Evaporation Forcing Factors of a Soil With a DSL

To analyze which forcing factors were able to explain the evaporation measured by the field lysimeter in 2012 and in 2015, the same procedure as used in CO_2 soil flux studies (e.g., Maier et al., 2010; Sánchez-Cañete et al., 2013) was used. First, all data was normalized to make them comparable, and high and low pass filtering were used to identify daily trends and long-term trends. Second, various hypotheses of possible mechanisms for water vapor transport through a DSL were tested. Third, a multivariate regression analysis was carried out for all possible forcing factors to identify the best model to explain the evaporation rates measured by the field lysimeter.

All weather forcing factors showed extreme variations in both mean and variances, as well as daily, synoptic (~7 days), and yearly variability. Therefore, all measurements were normalized and standardized as:

$$X_N = \frac{\left(X - \overline{X}\right)}{\sigma} \tag{1}$$

where X_N is the standardized variable, X the variable measurement, $\overline{X}$ the average of the variable over the period considered, σ is the standard deviation of the variable in the same period. Then, to study the correlations only at certain time scales, high and low pass filters were applied. A high pass filter extracts from a variable time series only the variations with period occurring below a certain time scale, so for example, a daily high pass filter, filters out the overall trend and all variations with the period longer than a day. A low pass filter does the opposite. The high pass filter used, was that proposed by Wilks (2006) for meteorological variables:

$$X_i = \frac{\left(X - \overline{X_i}\right)}{\sigma_i} \tag{2}$$

where X_i is the high pass filtered, standardized value for a time window of width i, $\overline{X_i}$ the running mean of X_i, and σ_i the standard deviation in the same time window i, which determines the time scale filtered; the i-values considered in this study were $i = 0.5$ days for daily and $i = 3$ days for synoptic time scales, following Sánchez-Cañete et al. (2013). The low pass filter used was the running mean itself; to be consistent with Equation 2 it was formulated as:

$$\overline{\overline{X}}_i = \frac{\left(\overline{X_i} - \overline{X}\right)}{\sigma} \tag{3}$$

To test various hypotheses of possible mechanisms of water vapor transport through a DSL, the correlation between the evaporation measured and the evaporation estimated by those mechanisms was studied for weather and lysimeter measurements. The possible mechanisms driving vapor fluxes considered in this study are: (a) isothermal liquid water flow (Equation 4); (b) diffusion (Equation 5); (c) soil temperature profile fluctuations (Equations 6 and 7); (d) wind speed (Equation 8); (e) daily cycles of condensation and evaporation of soil moisture in the DSL (Equation 9); and (f) atmospheric pressure fluctuation (Equation 10). Both Pearson and Spearman correlation coefficients were examined, to account for linear and nonlinear correlations. The corresponding equations used to calculate the evaporation rates predicted by each of these possible mechanisms are, respectively, as follows (see Supporting Information S1; Kuang et al., 2013):

$$E = f(E_p) \tag{4}$$

$$E = f(p_w) \tag{5}$$

$$\Delta_t E = f\left(\Delta_t\left(T_{\text{vap}} - T_0\right)\right) \tag{6}$$

$$\Delta_t E = f\left(\Delta_t\left(T_{\text{vap}} - T_0 - T_a\right)\right) \tag{7}$$

$$E = f(u) \tag{8}$$

$$E = f\left(p_w, \overline{u}\right) \tag{9}$$

$$E = f(|\Delta_t p_{\text{atm}}|) \tag{10}$$

where E is the evaporation rates measured by the lysimeter, E_p the potential evaporation calculated using Penman-Monteith (Monteith, 1980), Δ_t indicates the time differential of a variable, T_{vap} is the lysimeter and in situ soil temperature at vaporization plane, $\overline{u}$ is the daily average wind speed, and p_w is the vapor pressure, calculated as:

$$p_w = p_{\text{sat}}\,\text{RH} \tag{11}$$

where the saturated vapor pressure p_{sat} was calculated using Buck equation (Buck, 1981) as:

$$p_{\text{sat}} = 0.61121\exp\left(\left(18.678 - \frac{T_a}{234.5}\right)\left(\frac{T_a}{257.14 + T_a}\right)\right) \tag{12}$$

To fit a model to the E rates, multivariate regression analysis was conducted on all possible combinations of explanatory variables. The explanatory variables were ranked depending on their Pearson and Spearman correlation with E. The correlations and the regressions between the forcing factors and evaporation rates were calculated for the standardized forcing factors, for the filtered and standardized forcing factors, and for the time differentials of forcing factors, since the driver of the vapor transport could be the time derivative of the forcing factor instead of the magnitude of the forcing factor itself. Finally, the obtained multiple linear models were evaluated using the Nash-Sutcliffe efficiency coefficient (NSE), defined as:

$$\text{NSE} = 1 - \frac{\sum_{t=1}^{n}\left(X_0^t - X_m^t\right)^2}{\sum_{t=1}^{n}\left(X_0^t - \overline{X_0}\right)^2} \tag{13}$$

where X_0^t and X_m^t are the observed and modeled values at time t, respectively; $\overline{X_0}$ is the mean of the observed values; and n is the number of samples. The NSE can vary from $-\infty$ to 1, with 1 indicating a perfect match, 0 that the model predictions are not better than the mean, and negatives that the observed mean is a better predictor than the model (Du et al., 2018). Another way to evaluate the quality of a statistical model is to adjust the coefficient of determination R^2 by the number of explanatory variables used in the predictive model (Yin & Fan, 2001):

$$\overline{R}^2 = 1 - \left(1 - R^2\right)\frac{n-1}{n-p-1} \tag{14}$$

where p is the number of explanatory variables and n is sample size; the $\overline{R}^2$ can vary between 0 and 1, with 0 indicating no fit between the model and the observations, and 1 a perfect fit.

2.3. Simulation of the Lysimeter and In Situ Soil Evaporation With Hydrus1D

The Hydrus1D model (version 4.xx) accounting for coupled flow of heat, isothermal and thermal liquid water flow, and water vapor flow by diffusion (Saito et al., 2006), was used to estimate the evaporation rates from both, the lysimeter experiment and the in situ soil profile. The model input consisted of: (a) the environmental variables measured in the weather station as upper boundary conditions; (b) the soil parameters determined for laboratory lysimeter soil experiment (Balugani et al., 2021) and for the in situ soil (Balugani et al., 2017); (c) the measured in situ and lysimeter soil matric potentials and soil temperatures, for the initial conditions and for calibration purposes. The lower boundary conditions were set as: constant head boundary for the lysimeter in 2012, when the Mariotte bottle was working; no-flux boundary for the lysimeter in 2015, when the Mariotte bottle was flooded and acted as a closed bottom boundary; prescribed groundwater table depth for the in situ soil profile, measured hourly in a piezometer close to the in situ soil profile.

Finally, the evaporation rates estimated by Hydrus1D for the lysimeter where compared with the evaporation rates experimentally measured. Moreover, the resulting soil matric potential simulated by Hydrus1D was compared with lysimeter and in situ soil matric potential measurements, to test if Hydrus1D was able to simulate the formation of a DSL. The evaporation estimates obtained with the multivariate regression model (explained in Section 2.2) were also tested against the estimates from Hydrus1D for both, the lysimeter and in situ soil in 2012 and in 2015.

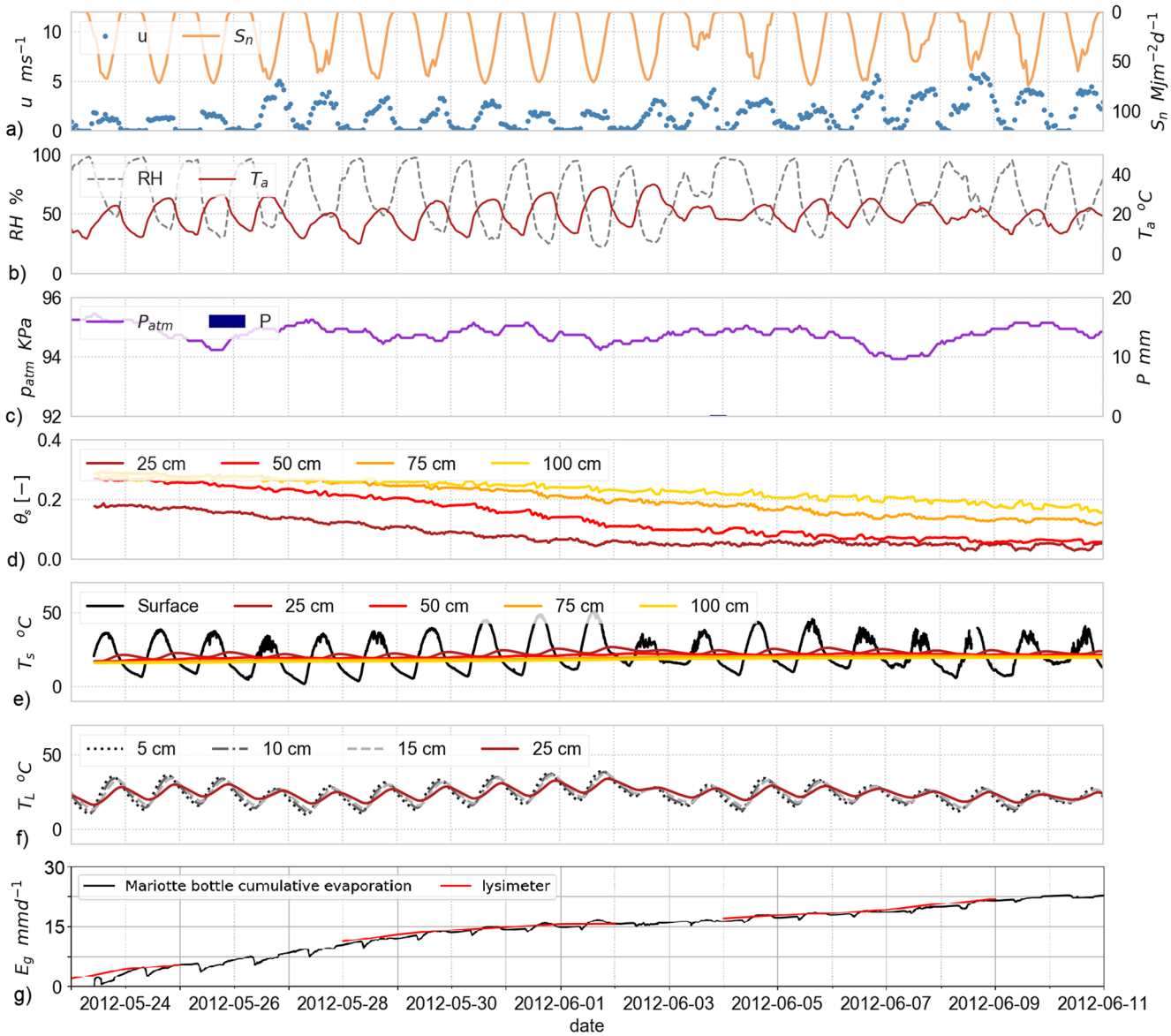

Figure 3. The data set of the dry season 2012 (23 May to 11 June): (a) wind speed (u) and net short wave radiation (S_n); (b) relative humidity (RH) and air temperature (T_a); (c) atmospheric pressure (p_{atm}) and precipitation (P); (d) in situ soil moisture ($\theta_{s,depth}$); (e) in situ soil temperature (T_s, depth); (f) lysimeter soil temperature ($T_{L,depth}$); (g) cumulative column groundwater evaporation (E_g) measured by the Lysimeter weighing system and the Mariotte bottle.

3. Results

3.1. Field Measurements

Figure 3 presents 19 days of dry season measurements (23 May to 11 June 2012) recorded by the weather station, the in situ soil profile and the lysimeter, at the start of the experiment, but after stabilization and testing of the setup. The hydrological year 2012 (1 October 2011 to 30 September 2012) was very dry with annual rainfall of only 312 mm. The 19-day analyzed were characterized by mostly clear sky with S_n reaching 70 Mj m^{-2} $days^{-1}$, u showing a daily pattern with no or very slow wind during the night and maximum speed (reaching 5 m s^{-1}) during the day (Figure 3a), large diurnal T_a and RH changes in order of 22°C and 75%, respectively (Figure 3b), no rain events and P_{atm} fluctuating between 94 and 95 KPa (Figure 3c). The in situ soil was drying up at the beginning of the experiment, and after 3 weeks the sensors at 25 and 50 cm depth showed dry soil (Figure 3d). The amplitude of diurnal soil temperature variations at the ground surface was larger (>30°C), but decreased rapidly with depth from ∼5°C at 25 cm to <1°C at 50 cm depth (Figure 3e). The lysimeter soil temperature ($T_{L,depth}$) showed

larger daily fluctuations at 25 cm depth than the in situ soil temperature ($T_{s,\text{depth}}$; Figures 3e and 3f). The in situ POT sensor reached its minimum matric potential value (−1.5 MPa, wilting point) on 26 May 2012, confirming the formation of an in situ DSL at least 22 cm thick. In contrast, the lysimeter soil was oven-dry at the start of the experiment ($Z_{\text{DSL}} = Z_{\text{WT}} - L_c = 70$ cm, with Z_{WT} the depth of the water table from the soil surface, and $L_c = 10$ cm as determined in Balugani et al., 2021; Clements & Wilkening, 1974) so the Mariotte bottle was discharging $E = E_g$ already from the beginning of the experiment, with average rate of 1.25 mm days^{-1} (as measured during the period 23 May to 11 June 2012; Figure 3g).

The years 2013 and 2014 were medium-wet, with yearly rainfalls 631, 682 mm respectively. The Mariotte bottle was filled with water by rain in November 2012 and remained full of water till the end of the experiment in 2015; therefore, due to the high water table in the lysimeter, it did not provide any meaningful data on evaporation. In the lysimeter, some drying was recorded only by the 5 cm deep matric potential sensor, and only during the summers of 2013 and 2014, showing that the soil reached field capacity, but no DSL was observed. In contrast, the in situ soil profile dried up every summer, with the 15 cm deep POT showing wilting point values in all years (2013–2015), and the 25 cm deep MPS1 sensor in the in situ soil profile reaching their minimum value (−500 kPa) at the beginning of June in years 2014 and 2015.

Figure 4 presents 19 days of dry season measurements (9–28 August 2015) recorded by the weather station, the in situ soil profile and the lysimeter, to be comparable with the measurements shown in Figure 3; both periods were representative of typical dry condition with similarly large vapor pressure deficit (large E_p) despite Figure 3 presenting the start of dry season and Figure 4 the end of dry season. The hydrological year 2015 was dry, with yearly rainfall of 322 mm; precipitation events stopped at the beginning of May, and the in situ profile and the lysimeter column soil moisture contents started to decrease. The 19-day analyzed were characterized by some cloud cover, with S_n reaching 70 Mj m^{-2} days^{-1} (Figure 4a), u showing a behavior similar to that of May–June 2012 (Figure 4a), large diurnal T_a and RH changes in order of 27°C and 75%, respectively, with the RH values lower than those recorded in 2012 (Figure 4b), two small rain events of 2 and 1 mm, and P_{atm} fluctuating between 93 and 94 KPa (Figure 4c). The in situ soil was already dry down to 75 cm depth at the beginning of the experiment, with the sensor at 100 cm depth showing ongoing drying (Figure 4d). The amplitude of diurnal soil temperature variations at the ground surface exceeding 40°C (Figure 4e) was even larger than in May–June 2012 (Figure 3e). During the spring 2015, the matric potential sensors in the lysimeter, at depths 5, 10, and 15 cm, showed continuous drying (not presented) down to maximum measurable dryness in the summer as seen in Figure 4f (sensors at 5 and 10 cm depth, i.e., within the DSL = 12 cm are not shown because highly negative), while in the lower lysimeter profile the sensors showed saturated soil conditions. The 2015 lysimeter evaporation measurements, showed weight changes similar to those recorded in the summer 2012, but with much thinner DSL (12 cm in 2015 while 70 cm in 2012; Figure 4g). The average evaporation rate measured between 9 and 28 August 2015 by the lysimeter weighing system was 1.05 mm days^{-1}, with measurement sensitivity lower than in 2012, implying, that the main evaporation trend was detected, but the daily fluctuations in weight were not observed. The measurements taken in the periods shown in Figures 3 and 4 have been used to calibrate (2012) and validate (2015) the statistical models presented in Sections 3.2.

3.2. Analysis of Forcing Factors for Evaporation From a Soil With a DSL

All the correlation tests between lysimeter measured E_g rates and evaporation estimated using Equations 4–10 were carried out for the 19-day period (23 May to 11 June 2012), as presented in Figure 3. All the correlation coefficients were very low, and the resulting models had NSE <0.16 for all processes. The average E_p was ∼7.5 mm days^{-1}; the evaporation predicted by diffusion alone, with a DSL 70 cm thick, was ∼0.05 mm days^{-1}, the evaporation predicted by atmospheric pressure fluctuations was ∼0.2 mm days^{-1}, so both much smaller than the observed mean of E_g ∼1.25 mm days^{-1}.

The preliminary correlation study for the multivariate regression analysis for all possible combinations of explanatory variables, showed that the Pearson coefficient was larger than 0.5 for $\Delta_t S_{n,0.5}$ and $\Delta_t T_{s,0,0.5}$ correlations with $E_{g,0.5}$, while the Spearman coefficient was larger than 0.4 for $\Delta_t T_{L,5,0.5}$, $\Delta_t T_{L,10,0.5}$, and $\Delta_t T_{L,15,0.5}$ correlations with $E_{g,0.5}$. The analysis carried out between the normalized explanatory variables and the evaporation rates showed no significant correlation improvement as compared to non-normalized variables. The measured evaporation rates show a distinct daily pattern, with minimum evaporation rates recurring regularly every 24 hr (Figure 5). The $E_{g,0.5}$ shows very low values around 9:00 a.m. local time (sunrise). This is the time at which T_L profile changed

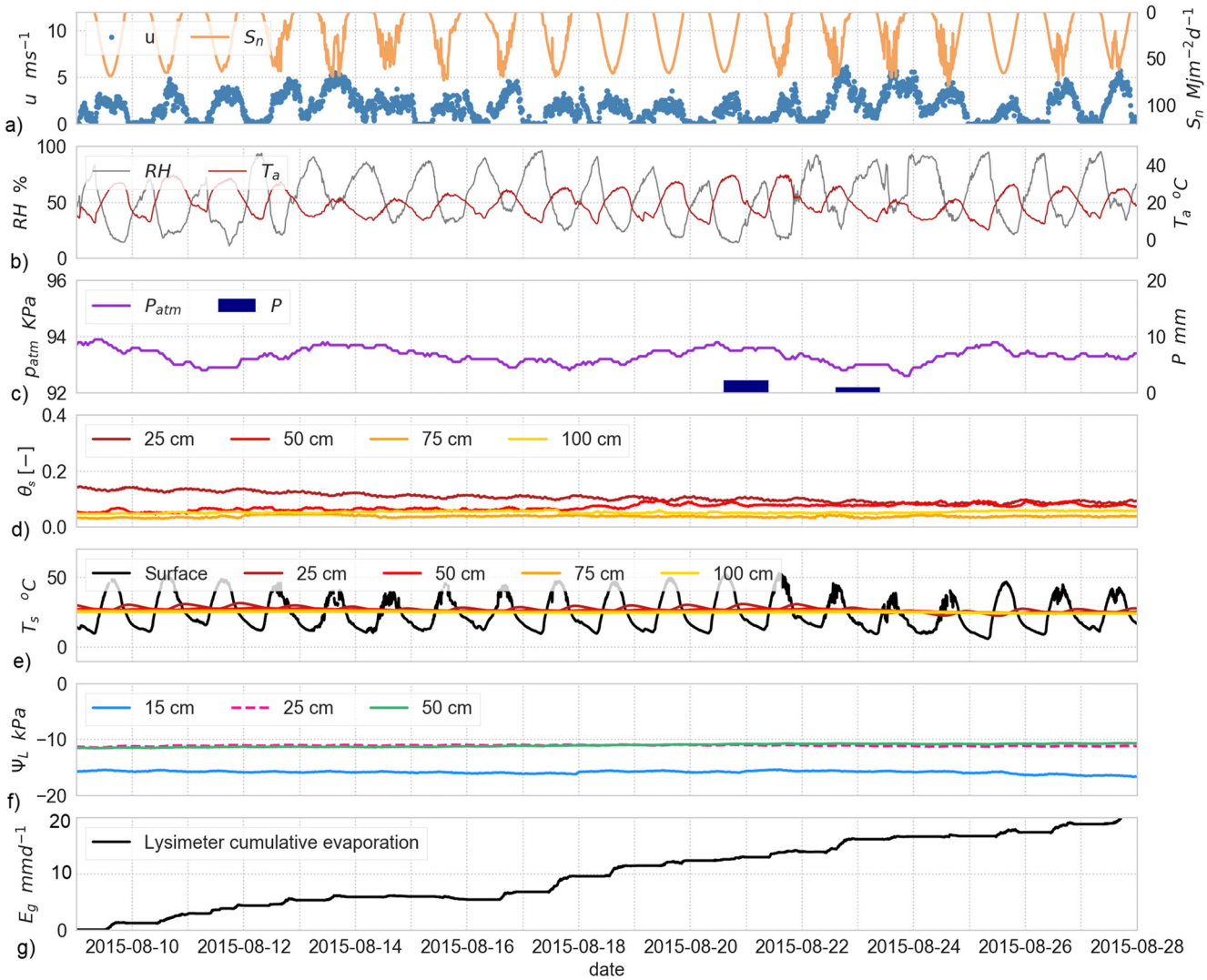

Figure 4. The data set of the dry season 2015 (9–28 August 2015): (a) wind speed (u) and net short wave radiation (S_n); (b) relative humidity (RH) and air temperature (T_a); (c) atmospheric pressure (p_{atm}) and precipitation (P); (d) in situ soil moisture ($\theta_{s,depth}$); (e) in situ soil temperature (T_s); (f) lysimeter soil matric potential (Ψ_L; sensors at depths 10 and 5 cm not shown because too negative); (g) lysimeter cumulative evaporation measurement.

shape by temperature increase within the upper 10 cm of soil. Between 9:00 and 19:00, the $E_{g,0.5}$ remained approximately constant, showing a local minimum between 16:00 and 18:00, which corresponded to the moment when the lysimeter temperature profile changed shape again, but with smaller gradient than in the morning. The $E_{g,0.5}$ reached another minimum at 22:00, which corresponded to the largest temperature difference between $T_{s,0}$ and $T_{L,5}$. Between 22:00 and 9:00, the $E_{g,0.5}$ rose gently (Figure 5a), and the lysimeter temperature profile remained stable with increasing temperature toward the deeper profile (Figure 5b).

The best multivariate regression model of both high and low pass filtered (daily) E_g was defined with S_n, $T_{s,0}$ and with the time differentials of $T_{L,\text{depth}}$ as predictors:

$$E_L = A_1 S_n + A_2 \Delta_t T_{s,0} + A_3 \Delta_t T_{L,5} + A_4 \Delta_t T_{L,10} + A_5 \Delta_t T_{L,15} + A_6 \Delta_t T_{L,25} + A_7 \quad (15)$$

where A_1, A_2, A_3, A_4, A_5, A_6, and A_7 are empirical coefficients fitted on the 2012 data, all significantly different from 0 (−0.46, −0.74, 1.79, −1.79, 1.45, −0.5, −0.06, respectively, p-value <0.001), with S_n, $T_{s,0}$ and $\Delta_t T_{L,5}$ accounting for 96% of the variance explained by the model. The resulting "E_L" model (Figure 5) had $\overline{R}^2 = 0.15$ and NSE = 0.52. The E_L model could not properly fit the very low $E_{g,0.5}$ values observed at ~9:00 (Figure 5). The residuals of the model were normally distributed, but their correlogram revealed an autocorrelation for

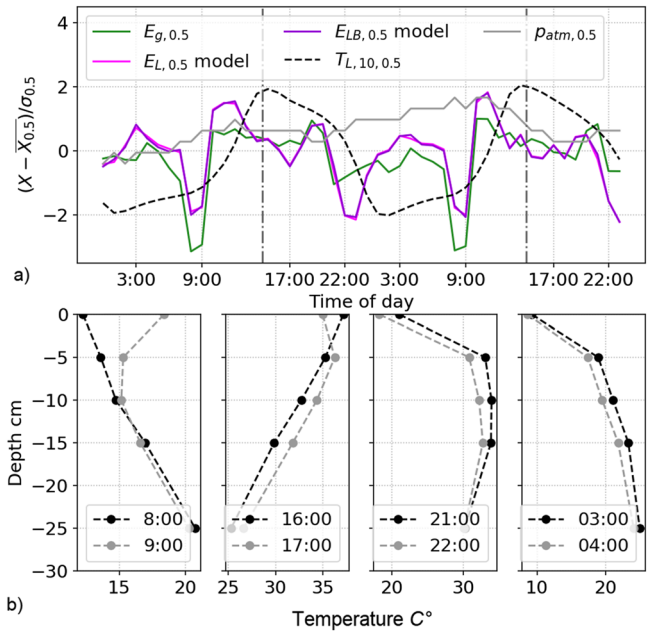

Figure 5. Daily variations of E_g rates (measured and estimated) and temperatures inside the lysimeter during the days 24 and 25 May 2012 following the local time: (a) standardized and filtered (high pass) for daily fluctuation lysimeter groundwater evaporation ($E_{g,0.5}$) rate, estimates of E_g obtained with the model presented by Equation 14 (E_L) and Equation 16 (E_{LB}) and soil temperature at 10 cm ($T_{L,10}$), solar noon is indicated with gray dotted lines; (b) temperatures measured in the lysimeter profile in different hours of the same days. Note that, in the Trabadillo study area, the local time is 2.5 hr ahead of the solar time.

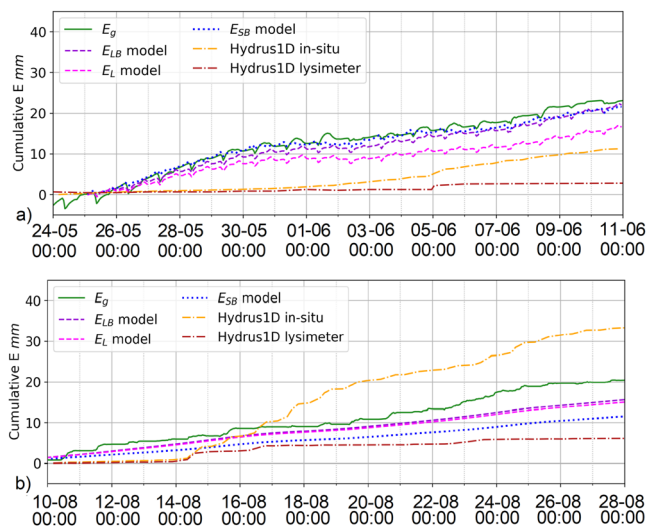

Figure 6. Measured cumulative E_g rates; evaporation rates predicted by the E_L model alone, in combination with the atmospheric pressure fluctuations model (E_{LB}), and using the E_{LB} model but for the in situ conditions (E_{SB}); and evaporation predicted by the Hydrus1D model for the lysimeter and the in situ soil profile, for (a) the calibration period (24 May to 11 June 2012) and (b) the validation period (17 August to 4 October 2015).

lags of 24 hr. This indicated that there were some other process(es) with a daily fluctuation, responsible for the daily variations of $E_{g,0.5}$. However, the correlation analysis, did not indicate any other possible explanatory variable(s) than those tested. The fitting of the model to the low and high pass filter variables, yielded $\overline{R}^2 = 0.52$ and NSE = 0.52 for the low pass filtered variables, and adjusted $\overline{R}^2 = 0.32$ and NSE = 0.33 for the high pass filtered variables.

The E_L model (Equation 15) accounts only for the DSL water vapor transport process caused by changes in the soil temperatures; this does not exclude the possibility that other processes contributed to the total water vapor transport. Since the laboratory experiment in Balugani et al. (2021) showed the relevance of the atmospheric pressure fluctuations, that effect was to be added to the E_L model. Balugani et al. (2021) calculated atmospheric pressure fluctuation effects as:

$$E = f(\Delta_t p_{\text{atm}}) = \begin{cases} |k_1^{\text{inverse}}(\Delta_t p_{\text{atm}})| + k_2, \Delta_t p_{\text{atm}} < 0 \\ |k_1^{\text{direct}}(\Delta_t p_{\text{atm}})| + k_2, \Delta_t p_{\text{atm}} \geq 0 \end{cases} \quad (16)$$

where k_1^{inverse} and k_1^{direct} are empirical coefficients, while inverse and direct refer to the type of correlation between evaporation rate and atmospheric pressure fluctuations. Finally Equation 16 was combined with Equation 15 to obtain the E_{LB} model (Figure 5), as:

$$E_{\text{LB}} = \begin{cases} |k_1^{\text{inverse}}(\Delta_t p_{\text{atm}})| + k_2 + E_L, \Delta_t p_{\text{atm}} < 0 \\ |k_1^{\text{direct}}(\Delta_t p_{\text{atm}})| + k_2 + E_L, \Delta_t p_{\text{atm}} \geq 0 \end{cases} \quad (17)$$

The E_{LB} model was applied to the soil in situ conditions to estimate evaporation there as well (E_{SB}).

3.3. Comparison Between Measured E_g and Evaporation Estimated Using Models E_L, E_{LB}, E_{SB}, and Hydrus1D

Figure 6 shows the experimentally measured cumulative E_g, the E_g estimated using the E_L and E_{LB} models (without and with atmospheric pressure fluctuations effect respectively), and the E_g estimated by the Hydrus1D, for the lysimeter and for the in situ soil profile in the calibration period from 24 May to 11 June 2012 (Figure 6a) and in the validation period from 9 to 28 August 2015 (Figure 6b; the E_{LB} model calculated for the in situ soil is called E_{SB}). The model calculations are displayed for only 18 days out of 19 from the data set, since the first half day is lost due to high filter processing.

In the calibration period (Figure 6a), the E_L and E_{LB} models follow very well the E_g measurements, after 18 days indicating cumulative values 16.7 and 22 mm respectively. The E_{LB} model only slightly underestimated E_g (by 0.5 mm after 19 days), while the E_L model clearly underestimated E_g (by 5.8 mm after 19 days). The Hydrus1D model was not able to simulate the lysimeter DSL properly, forming a layer of soil moisture close to residual soil moisture values (pseudo-DSL), only 5 cm thick, while the true DSL was 70 cm thick. That thin pseudo-DSL decreased the modeled evaporation rates so much that the estimated E_g after 18 days amounted to only 3 mm. The

Hydrus1D model simulation of the in situ conditions resulted in the formation of still thinner pseudo-DSL (only 1 cm); the E_g estimated by Hydrus1D model for the in situ soil was also very low, with cumulative E_g after 18 days estimated to be only 14 mm.

In the validation period, from 17 August to 4 October 2015 (Figure 6b), the E_L and E_{LB} models mostly follow the E_g measurements, after 18 days indicating cumulative values 16.5 and 17 mm respectively. The two models show very similar E_g estimates, both underestimating the measured E_g by 2.5 (E_L) and 2 mm (E_{LB}) after 18 days (so by ~0.1 mm days^{-1}). In 2015, the E_L and E_{LB} models predicted negligible variations in $E = E_g$, much smaller than those predicted by the calibration data set (Figure 6a). The Hydrus1D model, in the validation period, simulated the formation of a 1.5 cm thick pseudo-DSL for the lysimeter condition, and no DSL for the in situ condition (different than the 12 and 25 cm thick DSL measured), respectively. The E_g estimated by Hydrus1D model for the lysimeter was very low, just as in 2012, with cumulative E_g of 7 mm after 18 days. However, the E_g estimated by Hydrus1D model for the in situ soil was much larger than in 2012, being 32.4 mm, clearly overestimating the observed E_g.

4. Discussion

4.1. Measurements of Evaporation Through a Thick DSL and Comparison With Soil Profile Measurements

The setup of the lysimeter experiment and the use of oven-dry sand to fill it, implying the presence of a 70 cm thick DSL, and the lack of precipitation during summer 2012, guaranteed that the evaporation measured in that period originated from water table (E_g). The drying up of the upper DSL during maintenance in 2015 guarantees the same for summer 2015. The field lysimeter experiment showed that substantial E_g can take place even in the presence of a thick DSL, not only in laboratory conditions (Balugani et al., 2021) but also in field conditions. Besides, it also proved that the main process responsible was not diffusion as usually considered (e.g., in Hydrus1D, Saito et al., 2006). The lysimeter E_g in 2012 (1.25 mm days^{-1}) with 70 cm DSL, was similar to lysimeter E_g in 2015 (1.05 mm days^{-1}), measured with a naturally formed DSL of ~12 cm. This suggests that DSL thickness does not affect substantially the evaporation rates, at least when the DSL is ≥12 cm; however, due to different climatic conditions (early stage of dry season in 2012 vs. late in 2015), different initial conditions and also less sensitive lysimeter measurement in 2015, this latter statement requires further investigation. The fact that lysimeter E_g measured in May–June 2012 was larger than lysimeter E_g measured in August–September 2015 is likely due to the day duration, longer in the former case than in the latter, which resulted in larger $T_{s,0}$ variations during a day.

It should be pointed here that the presence of a DSL does not guarantee that $E \approx E_g$. The DSL develops depending on the evaporative conditions in the air above the soil and on the soil moisture conditions in the layer close to the soil surface. Whenever there is a dry period with no rain events and high E_p, a DSL may form at the soil surface. However, if the water table is deep enough so that the soil moisture profile is not at hydrostatic equilibrium (which is seldom the case in field conditions), the unsaturated zone below the DSL may contain water that can travel through capillary rise to the vaporization plane to evaporate from that plane by vapor transport through DSL to the surface (see Supporting Information S1). Such evaporation from the unsaturated zone would contribute to the total evaporation. However, in the two periods of the dry years 2012 and 2015 presented in this study, the situation was similar to that presented in Figure 1, that is, where the water table was very shallow and the matric potential sensors indicated that the soil moisture profile was close to hydrostatic equilibrium. Hence, in the periods shown in Figures 3 and 4, $E \approx E_g$.

The field lysimeter E_g rates were much higher than those observed by Balugani et al. (2021) in laboratory conditions despite the same setup, that is, 1.5 versus 0.3 mm days^{-1} respectively; the only differences were in different settings of upper boundary conditions, that is, controlled conditions in the laboratory lysimeter experiment and environmental conditions in the field lysimeter experiment. Even though the laboratory evaporative conditions were set similar to average field evaporative conditions, there were differences in atmospheric pressure (in absolute values and in fluctuations, see Section 4.2) and also in diurnal changes in RH, T_a, S_n, and u. The laboratory variations of RH, T_a, and S_n were dependent on the daily switching on and off of a radiative lamp, and u was changed only twice during the experiment. The field variations were random, driven by variability of weather conditions. In the laboratory condition, the main forcing factor of water vapor transport through the lysimeter DSL, was the atmospheric pressure fluctuation (Balugani et al., 2021) while in this field lysimeter study, the daily

temperature profile fluctuations were the dominant control, with the atmospheric pressure fluctuations playing a secondary role.

Other laboratory evaporation experiments with the formation of a DSL, conducted on small columns, showed measured evaporation rates (mostly driven by diffusion), around 0.5 mm days^{-1} (Lehmann et al., 2008; Shokri et al., 2008; Shokri & Or, 2011), so similar to the value measured with the lysimeter in laboratory condition by Balugani et al. (2021). Or et al. (2013) stated that the evaporation rates measured in the laboratory experiments, in the presence of a DSL, were independent of: (a) the upper boundary conditions; (b) soil properties; and (c) the evaporation rate before the formation of the DSL. Since the only difference between the field lysimeter set up of this study and the laboratory setup described in Balugani et al. (2021) was in different upper boundary conditions (which rejects the first assumption of Or et al., 2013), and because the field evaporation (1.25 mm days^{-1}) was much larger than the laboratory (0.3 mm days^{-1}), the field, upper boundary conditions must promote transport process or processes overlooked in the laboratory studies.

An interesting observation is that, despite very similar properties of the soil in the field lysimeter and in the nearby in situ profile, the formation of a DSL was more likely to occur in the in situ profile than in the nearby installed lysimeter. The in situ POT sensor reached values below wilting point every year, thus indicating development of a DSL even in the medium-wet years 2013 and 2014 when a DSL was not developed in the lysimeter. Considering the formation process of a DSL after a wet season, it has been observed, based on the POT data collected between 2010 and 2015 in the Trabadillo study area, that the in situ soil used to form a 15 cm thick DSL around mid-May, and the θ_{25} measurements showed that the soil was dry around the first week of June in all 4 yr, despite the fact that there were often some rain events in May (Balugani et al., 2017). The reason for the formation of the DSL in situ and not in the lysimeter in May were possibly: (a) transpiration by grasses (absent in the lysimeter); (b) good soil drainage (absent in the lysimeter); or (c) a combination of points (a) and (b).

4.2. Relevance of Different Transport Processes

The analysis of the drivers of the transport processes in the field lysimeter showed that the best explanatory variables of the E_g variations are the changes in the temperature profile inside the lysimeter:

$$E_g \sim \frac{\Delta T_L}{\Delta z\, \Delta t} \tag{18}$$

There are various possible processes that could explain the correlation in Equation 18. That process cannot be thermal flow of liquid water and water vapor in the soil (Section 2.2; Du et al., 2018; Saito et al., 2006), because in such case the water flux would depend on static, spatial differences in temperature in the soil, so the flux would be directed downwards during the day and upwards during the night (Zeng et al., 2011a, 2011b), which is the opposite to what was observed in the field. A possible process could be the cyclic condensation and evaporation of water in the DSL due to daily fluctuations in evaporative conditions at the lysimeter surface. The loss of water from the Mariotte bottle indicates loss of water from the saturated and/or capillary fringe (Figure 1), but the water vapor created at the vaporization plane can be accumulated in the DSL during the night and transported out of the lysimeter during the day. Such condensation and evaporation of water in the DSL has already been observed in field studies, where soil developed a DSL, even if only 1–5 cm thick (Assouline et al., 2013), and was able to enhance the overall water transport in such thin DSL. However, in this study, no correlation was found between the daily cycles of condensation and evaporation of soil moisture in the DSL and evaporation measured in the lysimeter (Section 3.2), and also no changes in soil matric potentials were observed through the lysimeter profile.

Another possible process taking place in the DSL is thermal convection, where temperature gradients result in natural convection of the gas phase in the soil (Kamai et al., 2009; Nachshon et al., 2008; Rose & Guo, 1995; Schubert & Schulz, 2002; Weisbrod et al., 2009; Witkamp, 1969). Ganot et al. (2014) studied the effects of thermal convection on CO_2 soil respiration using soil columns with a design similar to that presented in this study, and found that thermal convection was relevant in the presence of soil aggregates and not in the presence of loose sand (due to the relatively high Rayleigh-Darcy number of the sand). However, Roland et al. (2015) measured statistically significant correlation between sandy-loam CO_2 soil respiration rates, temperature profile in the soil, and solar radiation. They concluded that, under certain u regimes, changes in T_s driven by S_n can affect bulk air transport in a soil. Since $T_{s,0}$, T_L, and S_n were also strongly correlated with u, it was not possible to assess the separated effects of u regimes that would result in a strong coupling of gas transport with $T_{s,0}$, which they did

not measure. In this study, that coupling was confirmed. The theory of bulk air transport related to S_n and $T_{s,0}$ is also supported by the direct observation of strong dust devils in the study area during fieldwork, and by infrared camera images, showing the temperature at the soil surface changing in patches, at a rate as high as 3°C min^{-1} (not shown here).

The Hydrus1D model was not able to simulate properly the presence of a DSL in the periods studied (Figure 6), simulating only thin (5–1.5 cm thick) pseudo-DSL, where the soil moisture was close to its residual values, and water moved mainly as vapor by diffusion only. This limited the evaporation flow estimated by Hydrus1D for the lysimeter to values such as 0.17 and 0.39 mm $days^{-1}$ in 2012 and 2015, respectively, that is, significantly smaller than observed experimentally. In the Hydrus1D simulation of the in situ soil evaporation for the year 2012, the initial conditions were set as observed in the field, with an initial pseudo-DSL 15 cm thick (Section 3.3), which was reduced in the simulation to a thickness of 1 cm due to upward liquid water fluxes. This 1 cm thick, simulated pseudo-DSL, however, was enough to limit the Hydrus1D estimated evaporation rates to 0.78 mm $days^{-1}$. Conversely, in the Hydrus1D simulation of in situ soil evaporation in 2015, the soil initial conditions were relatively wet (the simulation was started at the beginning of May), and a pseudo-DSL did not form, despite the very dry weather conditions. Therefore, the main water flow in Hydrus1D 2015 simulation was isothermal liquid water flow, so that evaporation rates estimated by Hydrus1D were much larger than those in 2012 (2.06 mm $days^{-1}$). This supports the idea that Hydrus1D is not suited to properly model the measured evaporation rates in very dry soil conditions with DSL, as previously suggested by Balugani et al. (2017).

The descriptive models based on diffusion, thermal fluxes, or daily cycles of condensation and evaporation of soil moisture in the DSL (Equations 5, 7, and 9, respectively), did not estimate evaporation rates better than the E_L and E_{LB} models, as they had lower NSE scores than both E_L and E_{LB} models. The low correlation between measured evaporation rates and the forcing factors of these transport processes (diffusion, thermal fluxes, or daily cycles of condensation and evaporation of soil moisture in the DSL) may be due to: (a) the unknown interaction between different processes resulting in a nonlinear dependence of evaporation rates on different forcing factors; or (b) the larger effect of the main process (bulk air transport driven by solar radiation), hiding the effect of other physical processes. The interconnectedness and complexity of different evaporation processes in dry soil is recognized in the scientific literature (Brutsaert, 2014a, 2014b; Vanderborght et al., 2017); one way these processes can interact, is for example, by having wind speed and atmospheric pressure fluctuations actively pumping out air from the first centimeters of a soil (Auer et al., 1996; Balugani et al., 2021; Stauffer et al., 1997), effectively decreasing the travel distance of other DSL transport processes (Auer et al., 1996; Davarzani et al., 2014). The way in which the transport processes interact is likely affected by: (a) DSL thickness, for example, when DSL thickness is shorter than the depth from which air can be removed by wind speed or atmospheric pressure changes; (b) soil material properties, which are usually uncertain and heterogeneous in the field conditions; and (c) weather conditions, with forcing factors having different magnitudes in different climates. The inclusion of transport processes that operate at larger depths can help to explain observed evaporation rates in dry environmental conditions.

The fact that, in this field study, the main forcing factor driving the transport of the gas phase in the DSL is different than that in the laboratory conditions (Balugani et al., 2021) despite an identical columnar setup, is indicative of how complex the DSL evaporation can be. Under laboratory conditions, the main forcing factor driving vapor transport through the DSL was the atmospheric pressure fluctuation. In the field experiment, p_{atm} was smaller than in the laboratory experiment, both in magnitude and in variation. The difference in p_{atm} magnitude, due to the different altitudes above the mean sea level (~9 m a.s.l. and p_{atm} ~100 kPa in Wageningen, the Netherlands against ~790 m a.s.l. and ~92 kPa of Trabadillo, Spain) is not expected to have had a relevant impact on evaporation rates. However, the difference in p_{atm} variations between the Netherlands and Spain (with average amplitudes of 6 and 3 kPa in Wageningen and in Trabadillo, respectively), resulted in E_g estimated using Equation 16 for Trabadillo being half of that in Wageningen. The estimated E_g contribution due to atmospheric pressure fluctuations in the Trabadillo site (~0.2 mm $days^{-1}$) was also several times lower than the measured E_g rate. However, the inclusion of the atmospheric pressure fluctuations in the E_{LB} model, improved the E_L model estimates of E_g, indicating that the evaporation process was probably dominated by profile temperature fluctuations (Equation 15), with a less distinct but significant effect of atmospheric pressure fluctuation (Equation 16). The dominance of the profile temperature fluctuations as forcing factor of the evaporation in this field study, explains why there was very little correlation between E_g and p_{atm}.

4.3. Limitations and Further Studies

We assume that the loss of water from the Mariotte bottle represented the loss of water from the saturated soil inside the lysimeter (E_g) in 2012, when both lysimeter and Mariotte bottle measurements were available. This assumption is based on the fact that: (a) both the Mariotte bottle and the soil column are weighed continuously, and thus it is possible to assess whether water is lost from the lysimeter-Mariotte bottle system or not; (b) there was no leakage in the Mariotte bottle-lysimeter system; (c) when the surface of the lysimeter was covered, the loss of weight in the Mariotte bottle dropped in less than 30 min; (c) the lysimeter was left in the field, covered, for 6 days, then 9 days with no coverage, to equilibrate before starting the experiment. Since the water that exits the Mariotte bottle goes to the saturated zone in the lysimeter, since initially the sand was oven-dry, since there is an equal net loss of water from the lysimeter as measured by both weighing systems, and since this loss of water can take place only at the lysimeter upper boundary, we state that the water loss from the Mariotte bottle was lost as E_g. The Mariotte bottle was completely filled with water in 2015, and thus the evaporation measurements came from the lysimeter weighing system only; the results show evaporation in line with what was observed in 2012, and the E_{LB} model could estimate the observations satisfactorily well.

A possible limit to this approach is that the accuracy of the lysimeter weighing system is lower than the accuracy of the Mariotte bottle system. However, the E_L and E_{LB} models were able to properly estimate the evaporation rates in 2015 as well, when only lysimeter weigh data were available, thus showing the robustness of the model, at least for the specific conditions of the experiment presented in this study. The mechanism of groundwater evaporation in the lysimeter is as follows: the water lost at the vaporization plane (in the unsaturated zone) is quickly replaced by water lost at the water table (in the saturated zone), so that the evaporated water is affecting the balance of the saturated zone, not that of the unsaturated zone. Possible short-time fluctuations in the unsaturated zone water content profile either balance out (resulting in zero net change in water content stored in the unsaturated zone) or do eventually affect the saturated zone, as the comparison between the lysimeter weigh and the Mariotte bottle weigh shows.

Finally, we want to address the complications of handling transient conditions in the field, and more specifically their effect on the Mariotte bottle measurements. Even though the daily loss of water from the Mariotte bottle is interpreted as E_g, it is certainly possible that the hourly changes (and daily fluctuations) in the pressure head inside the lysimeter exist, and thus in the water extracted from the Mariotte bottle, which could be due to simple fluctuations of atmospheric pressure or earth tides, resulting in zero net evaporation from the lysimeter (see explanation in Balugani et al., 2021). That is the reason we tested the correlation between the explanatory variables and the Mariotte bottle weight change, using low and high pass filters, in order to study whether the explanatory variables were able to describe the daily fluctuations in Mariotte bottle weigh only, the long term trend in water loss from the Mariotte bottle weigh only, or both. Even though the E_L and E_{LB} models performed better in predicting the daily fluctuations only (NSE = 0.52) than the long-term trend (NSE = 0.33), the model performance for the unfiltered evaporation rates was satisfactory (NSE = 0.52), as well as the prediction of the model for cumulative evaporation for both 2012 and 2015.

It should be noted that none of the multiple linear regressions was able to properly model the low evaporation rates values recorded every day between 8:00 and 9:15 a.m. of local time (~2.5 hr ahead of solar time) and coincident with sunrise (Figure 5). These low values are not due to temperature effects on the load cell sensor, since they were already corrected for; also the weight measurements were taken every minute and averaged and recorded every 5 min, making them reliable. Looking at Figure 5, it seems that these low values are somehow related to the change in T_L gradient in the first 5 or 10 cm of the lysimeter, probably due to disruption of the temperature-related transport process during sunrise. It is possible that one of the transport mechanisms at play in the DSL, is dependent on a temperature gradient in the soil profile; the transport mechanism is then disrupted whenever the gradient between $T_{s,0}$ and $T_{L,5}$ becomes zero and, eventually, reverses.

5. Conclusions

The field lysimeter system employed in this study was able to measure soil evaporation in the presence of a DSL, and to measure separately groundwater and unsaturated zone evaporation, as defined in Balugani et al. (2016). Groundwater evaporation (E_g) measured in a soil with 70 cm DSL was ~5 times higher than in the similar experiment conducted in the laboratory conditions in the Netherlands with the same lysimeter setup (~1.25 mm days^{-1}

in 2012 and 1.05 mm days^{-1} in 2015 vs. ∼0.3 mm days^{-1} respectively). The dominant forcing factor best explaining variation in the E_g rates measured in this study were the temperature profile fluctuations in the lysimeter, as related to changes in solar radiation (E_L model); the atmospheric pressure fluctuation, which was the dominant forcing factor for evaporation in the laboratory conditions, contributed only to 13% of the measured E_g (0.2 mm days^{-1}) in field conditions. However, the addition of the atmospheric pressure fluctuation effect to the E_L model, resulting in the E_{LB} model, improved the E_g estimate in the field lysimeter experiment.

The evaporation rates measured in the lysimeter with a DSL were much larger than those estimated using hydrology models based on liquid water flow and vapor transport by only diffusion such as Hydrus1D model. When applied to the in situ conditions, the E_{LB} model gives results that are not as wildly affected by groundwater depth as those of Hydrus1D; this brings the estimates of the E_{LB} model with previous observations in the area (Balugani et al., 2017). In order to improve evaporation estimates in the presence of a DSL, further studies are required to (a) determine the most important transport processes in the DSL as a function of DSL thickness, and (b) to include the unaccounted, relevant transport processes in hydrological models of soil evaporation.

List of Symbols and Abbreviations

Δ_z: depth differential (between the vaporization plane and the soil/lysimeter surface)
Δ_t: time differential
$\theta_{s,\mathrm{depth}}$: soil moisture measured in the in situ soil profile
σ: standard deviation
σ_i: moving standard deviation with time window i
$\Psi_{L,\mathrm{depth}}$: matric potential measured in the lysimeter soil
$\Psi_{s,\mathrm{depth}}$: matric potential measured in the in situ soil
$A_1, A_2, \ldots, A_7$: empirical coefficients
DSL: dry soil layer
E: evaporation rate
E_p: evaporative potential rate
E_u: unsaturated zone evaporation rate
E_g: groundwater evaporation rate
E_L: evaporation model using changes in the lysimeter soil temperatures
E_{LB}: E_L model with atmospheric pressure fluctuations for lysimeter soil
E_{SB}: E_L model with atmospheric pressure fluctuations for in situ soil
i: width of time window (in days)
$k_1^{\mathrm{inverse}}, k_1^{\mathrm{direct}}, k_2$: empirical parameters
L_c: critical length
n: number of samples in a statistic
NSE: Nash-Sutcliffe efficiency coefficient
P: precipitation
p: number of explanatory variables
p_{atm}: atmospheric pressure
p_{sat}: saturated vapor pressure
p_w: vapor pressure above the soil/lysimeter surface
POT: polymeric tensiometer
R^2: coefficient of determination
$\overline{R}^2$: coefficient of determination adjusted for number of explanatory variables
RH: relative humidity
S_n: net short wave radiation
t: time
T_a: air temperature measured at 2 m height
T_0: surface temperature, same for lysimeter and in situ soil profile
$T_{L,\mathrm{depth}}$: temperature measured in the lysimeter
$T_{s,\mathrm{depth}}$: temperature measured in the in situ soil profile
$T_{s,\mathrm{vap}}$: in situ soil temperature at vaporization plane

$T_{L,\mathrm{vap}}$: lysimeter soil temperature at vaporization plane
u: wind speed
$\overline{u}$: wind speed averaged over a day
X: a given variable
$\overline{X}$: average of a given variable over the period considered
X_i: high pass filtered for a time window of width i of a given variable
$\overline{X_i}$: the running mean for a time window of width i of a given variable
$\overline{\overline{X}}_i$: low pass filtered for a time window of width i of a given variable
X_m^t: modeled value of a variable at time t
X_0^t: observed value of a variable at time t
$\overline{X_0}$: the mean of the observed variable over the whole experiment
X_N: normalized and standardized of a given variable
Z_{WT}: depth of water table from soil surface
Z_{DSL}: depth of DSL from soil surface

Data Availability Statement

Data (Balugani, 2022) used in this study are deposited on Mendeley with https://doi.org/10.17632/gp9ff6vks3.1. The Data has not been published before in any other research article.

Acknowledgments
This research was funded by the International Institute for Geo-Information Science and Earth Observation (ITC), faculty of Twente University (the Netherlands). The authors thank the Department of Environmental Sciences in Wageningen University (WUR), for the preparation of the column experiment. The authors thank the three anonymous reviewers and the Water Resources Research editorial team (Editor Peter Troch and an anonymous Associate Editor) for the constructive and helpful comments.

References

Assouline, S., Tyler, S. W., Selker, J. S., Lunati, I., Higgins, C. W., & Parlange, M. B. (2013). Evaporation from a shallow water table: Diurnal dynamics of water and heat at the surface of drying sand. *Water Resources Research*, *49*(7), 4022–4034. https://doi.org/10.1002/wrcr.20293

Auer, L. H., Rosenberg, N. D., Birdsell, K. H., & Whitney, E. M. (1996). The effects of barometric pumping on contaminant transport. *Journal of Contaminant Hydrology*, *24*(2), 145–166. https://doi.org/10.1016/S0169-7722(96)00010-1

Bakker, G., van der Ploeg, M. J., de Rooij, G. H., Hoogendam, C. W., Gooren, H. P. A., Huiskes, C., et al. (2007). New polymer tensiometers: Measuring matric pressures down to the wilting point. *Vadose Zone Journal*, *6*(1), 196–202. https://doi.org/10.2136/vzj2006.0110

Balugani, E. (2022). Lysimeter and in situ field experiments to study soil evaporation through a dry soil layer under semi-arid climate [Dataset]. Mendeley Data, V1. https://doi.org/10.17632/gp9ff6vks3.1

Balugani, E., Lubczynski, M. W., & Metselaar, K. (2016). A framework for sourcing of evaporation between saturated and unsaturated zone in bare soil condition. *Hydrological Sciences Journal*, *61*(11), 1981–1995. https://doi.org/10.1080/02626667.2014.966718

Balugani, E., Lubczynski, M. W., & Metselaar, K. (2021). Evaporation through a dry soil layer: Column experiments. *Water Resources Research*, *57*(8), 1–14. https://doi.org/10.1029/2020WR028286

Balugani, E., Lubczynski, M. W., Reyes-Acosta, L., van der Tol, C., Francés, A. P., & Metselaar, K. (2017). Groundwater and unsaturated zone evaporation and transpiration in a semi-arid open woodland. *Journal of Hydrology*, *547*, 54–66. https://doi.org/10.1016/j.jhydrol.2017.01.042

Balugani, E., Lubczynski, M. W., van der Tol, C., & Metselaar, K. (2018). Testing three approaches to estimate soil evaporation through a dry soil layer in a semi-arid area. *Journal of Hydrology*, *567*, 405–419. https://doi.org/10.1016/j.jhydrol.2018.10.018

Bowling, D. R., Egan, J. E., Hall, S. J., & Risk, D. A. (2015). Environmental forcing does not induce diel or synoptic variation in the carbon isotope content of forest soil respiration. *Biogeosciences*, *12*(16), 5143–5160. https://doi.org/10.5194/bg-12-5143-2015

Brutsaert, W. (2014a). Daily evaporation from drying soil: Universal parameterization with similarity. *Water Resources Research*, *50*(4), 3206–3215. https://doi.org/10.1002/2013WR014872.Received

Buck, A. L. (1981). New equations for computing vapor pressure and enhancement factor. *Journal of Applied Meteorology*, *20*(12), 1527–1532. https://doi.org/10.1175/1520-0450(1981)020<1527:nefcvp>2.0.co;2

Clements, W. E., & Wilkening, M. H. (1974). Atmospheric pressure effects on ^{222}Rn transport across the Earth-air interface. *Journal of Geophysical Research*, *79*(33), 5025–5029. https://doi.org/10.1029/JC079i033p05025

Daoud, M. G., Lubczynski, M. W., Vekerdy, Z., & Francés, A. P. (2022). Application of a novel cascade-routing and reinfiltration concept with a Voronoi unstructured grid in MODFLOW 6, for an assessment of surface-water/groundwater interactions in a hard-rock catchment (Sardon, Spain). *Hydrogeology Journal*, *30*(3), 899–925. https://doi.org/10.1007/s10040-021-02430-z

Davarzani, H., Smits, K., Tolene, R. M., & Illangasekare, T. (2014). Study of the effect of wind speed on evaporation from soil through integrated modeling of the atmospheric boundary layer and shallow subsurface. *Water Resources Research*, *50*(1), 661–680. https://doi.org/10.1002/2013WR013952

Deol, P. K., Heitman, J. L., Amoozegar, A., Ren, T., & Horton, R. (2014). Inception and magnitude of subsurface evaporation for a bare soil with natural surface boundary conditions. *Soil Science Society of America Journal*, *78*(5), 1544–1551. https://doi.org/10.2136/sssaj2013.12.0520

Dijkema, J., Koonce, J. E., Shillito, R. M., Ghezzehei, T. A., Berli, M., Ploeg Van Der, M. J., & Van Genuchten, M. T. (2017). Water distribution in an arid zone soil: Numerical analysis of data from a large weighing lysimeter. https://doi.org/10.2136/vzj2017.01.0035

Du, C., Yu, J., Wang, P., & Zhang, Y. (2018). Analyzing the mechanisms of soil water and vapor transport in the desert vadose zone of the extremely arid region of northern China. *Journal of Hydrology*, *558*, 592–606. https://doi.org/10.1016/j.jhydrol.2017.09.054

Farrell, D. A., Greacen, E. L., & Gurr, C. G. (1966). Vapor transfer in soil due to air turbulence. *Soil Science*, *102*(5), 305–313. https://doi.org/10.1097/00010694-196611000-00005

Fetzer, T., Vanderborght, J., Mosthaf, K., Smits, K. M., & Helmig, R. (2017). Heat and water transport in soils and across the soil-atmosphere interface: 2. Numerical analysis. *Water Resources Research*, *53*, 1080–1100. https://doi.org/10.1002/2016WR019982.Heat

Francés, A. P., Lubczynski, M. W., Roy, J., Santos, F. A. M., & Mahmoudzadeh Ardekani, M. R. (2014). Hydrogeophysics and remote sensing for the design of hydrogeological conceptual models in hard rocks Sardón catchment (Spain). *Journal of Applied Geophysics*, *110*, 63–81. https://doi.org/10.1016/j.jappgeo.2014.08.015

Francés, A. P., Su, Z., & Lubczynski, M. W. (2015). Integration of hydrogeophysics and remote sensing with coupled hydrological models.
Ganot, Y., Dragila, M. I., & Weisbrod, N. (2014). Impact of thermal convection on CO_2 flux across the earth-atmosphere boundary in high-permeability soils. *Agricultural and Forest Meteorology*, *184*, 12–24. https://doi.org/10.1016/j.agrformet.2013.09.001
Hassan, S. M. T., Lubczynski, M. W., Niswonger, R. G., & Su, Z. (2014). Surface-groundwater interactions in hard rocks in Sardon Catchment of western Spain: An integrated modeling approach. *Journal of Hydrology*, *517*, 390–410. https://doi.org/10.1016/j.jhydrol.2014.05.026
Kamai, T., Weisbrod, N., & Dragila, M. I. (2009). Impact of ambient temperature on evaporation from surface-exposed fractures. *Water Resources Research*, *45*(2). https://doi.org/10.1029/2008WR007354
Kuang, X., Jiao, J. J., & Li, H. (2013). Review on airflow in unsaturated zones induced by natural forcings. *Water Resources Research*, *49*(10), 6137–6165. https://doi.org/10.1002/wrcr.20416
Lehmann, P., Assouline, S., & Or, D. (2008). Characteristic lengths affecting evaporative drying of porous media. *Physical Review E—Statistical, Nonlinear and Soft Matter Physics*, *77*(5), 1–16. https://doi.org/10.1103/PhysRevE.77.056309
Lehmann, P., & Or, D. (2009). Evaporation and capillary coupling across vertical textural contrasts in porous media. *Physical Review E*, *80*(4), 46318. https://doi.org/10.1103/physreve.80.046318
Lubczynski, M. W., & Gurwin, J. (2005). Integration of various data sources for transient groundwater modeling with spatio-temporally variable fluxes—Sardon study case, Spain. *Journal of Hydrology*, *306*(1–4), 71–96. https://doi.org/10.1016/j.jhydrol.2004.08.038
Ma, Z., Wang, W., Zhang, Z., Brunner, P., Wang, Z., Chen, L., et al. (2019). Assessing bare-soil evaporation from different water-table depths using lysimeters and a numerical model in the Ordos Basin, China. *Hydrogeology Journal*, *27*(7), 2707–2718. https://doi.org/10.1007/s10040-019-02012-0
Maier, M., Schack-Kirchner, H., Hildebrand, E. E., & Holst, J. (2010). Pore-space CO_2 dynamics in a deep, well-aerated soil. *European Journal of Soil Science*, *61*(6), 877–887. https://doi.org/10.1111/j.1365-2389.2010.01287.x
Monteith, J. L. (1980). The development and extension of Penman's. evaporation formula. In D. Hillel (Ed.), *Application of soil physics*. Apress.
Mukherjee, S., Mishra, A., & Trenberth, K. E. (2018). Climate change and drought: A perspective on drought indices. *Current Climate Change Reports*, *4*(2), 145–163. https://doi.org/10.1007/s40641-018-0098-x
Nachshon, U., Weisbrod, N., & Dragila, M. I. (2008). Quantifying air convection through surface-exposed fractures: A laboratory study. *Vadose Zone Journal*, *7*(3), 948–956. https://doi.org/10.2136/vzj2007.0165
Or, D., Lehmann, P., Shahraeeni, E., & Shokri, N. (2013). Advances in soil evaporation physics—A review. *Vadose Zone Journa*l, *12*(4). https://doi.org/10.2136/vzj2012.0163
Parsons, A. J., & Abrahams, A. D. (1994). Geomorphology of desert environments. In A. D. Abrahams & A. J. Parsons (Eds.), *Geomorphology of desert environments*. Springer. https://doi.org/10.1007/978-94-015-8254-4_1
Philip, J. R., & de Vries, V. D. (1957). Moisture movement in porous materials under temperature gradient. *Eos, Transactions American Geophysical Union*, *38*(2), 222–232. https://doi.org/10.1029/tr038i002p00222
Reyes-Acosta, J. L., & Lubczynski, M. W. (2014). Optimization of dry-season sap flow measurements in an oak semi-arid open woodland in Spain. *Ecohydrology*, *7*(2), 258–277. https://doi.org/10.1002/eco.1339
Roland, M., Vicca, S., Bahn, M., Ladreiter-Knauss, T., Schmitt, M., & Janssens, I. A. (2015). Importance of nondiffusive transport for soil CO_2 efflux in a temperate mountain grassland. *Journal of Geophysical Research: Biogeosciences*, *120*(3), 502–512. https://doi.org/10.1002/2014JG002788
Rose, A. W., & Guo, W. (1995). Thermal-convection of soil air on hillsides. *Environmental Geology*, *25*, 258–262. https://doi.org/10.1007/bf00766755
Saito, H., Simunek, J., & Mohanty, B. P. (2006). Numerical analysis of coupled water, vapor, and heat transport in the vadose zone. *Vadose Zone Journal*, *5*(2), 784–800. https://doi.org/10.2136/vzj2006.0007
Sánchez-Cañete, E. P., Kowalski, A. S., Serrano-Ortiz, P., Pérez-Priego, O., & Domingo, F. (2013). Deep CO_2 soil inhalation/exhalation induced by synoptic pressure changes and atmospheric tides in a carbonated semiarid steppe. *Biogeosciences*, *10*(10), 6591–6600. https://doi.org/10.5194/bg-10-6591-2013
Schlaepfer, D. R., Bradford, J. B., Lauenroth, W. K., Munson, S. M., Tietjen, B., Hall, S. A., et al. (2017). Climate change reduces extent of temperate drylands and intensifies drought in deep soils. *Nature Communications*, *8*(1), 14196. https://doi.org/10.1038/ncomms14196
Schubert, M., & Schulz, H. (2002). Diurnal radon variations in the upper soil layers and at the soil-air interface related to meterological parameters. *Health Physics*, *83*(1), 91–96. https://doi.org/10.1097/00004032-200207000-00010
Scotter, D. R., & Raats, P. A. C. (1969). Dispersion of water vapor n soil due to air turbulence. *Soil Science*, *108*(3), 170–176. https://doi.org/10.1097/00010694-196909000-00004
Shokri, N., Lehmann, P., Vontobel, P., & Or, D. (2008). Drying front and water content dynamics during evaporation from sand delineated by neutron radiography. *Water Resources Research*, *44*(6). https://doi.org/10.1029/2007wr006385
Shokri, N., & Or, D. (2011). What determines drying rates at the onset of diffusion controlled stage-2 evaporation from porous media? *Water Resources Research*, *47*(9), 1–8. https://doi.org/10.1029/2010WR010284
Shokri, N., & Salvucci, G. D. (2011). Evaporation from porous media in the presence of a water table. *Vadose Zone Journal*, *10*(4), 1309–1318. https://doi.org/10.2136/vzj2011.0027
Simunek, J., van Genuchten, M. T., & Sejna, M. (2008). Development and applications of the HYDRUS and STANMOD software packages and related codes. *Vadose Zone Journal*, *7*(2), 587–600. https://doi.org/10.2136/vzj2007.0077
Stauffer, P. H., Auer, L. H., & Rosenberg, N. D. (1997). Compressible gas in porous media: A finite amplitude analysis of natural convection. *International Journal of Heat and Mass Transfer*, *40*(7), 1585–1589. https://doi.org/10.1016/S0017-9310(96)00222-0
Vanderborght, J., Helmig, R., Fetzer, T., Mosthaf, K., & Smits, K. M. (2017). Heat and water transport in soils and across the soil-atmosphere interface: 1. Theory and different model concepts. *Water Resources Research*, *53*(2), 1057–1079. https://doi.org/10.1002/2016WR019983.Heat
Vanderborght, J., Shahraeeni, E., Pohlmeier, A., Merz, S., Jonard, F., Graf, A., et al. (2014). Monitoring of soil evaporation and drying at different scales. Retrieved from http://juser.fz-juelich.de/record/172374
Wang, X. (2015). Vapor flow resistance of dry soil layer to soil water evaporation in arid environment: An overview. *Water*, *7*(8), 4552–4574. https://doi.org/10.3390/w7084552
Webb, S. W., & Ho, C. K. (1998). Review of enhanced vapor diffusion in porous media. SAND-98-1819C; CONF-980559.
Weisbrod, N., Dragila, M. I., Nachshon, U., & Pillersdorf, M. (2009). Falling through the cracks: The role of fractures in Earth-atmosphere gas exchange. *Geophysical Research Letters*, *36*(2), L02401. https://doi.org/10.1029/2008gl036096
Wilks, D. S. (2006). *Statistical methods in the atmospheric sciences* (2nd ed.). Academic Press.
Witkamp, M. (1969). Cycles of temperature and carbon dioxide evolution from litter and soil. *Ecology*, *50*(5), 922–924. https://doi.org/10.2307/1933713

Xu, C., McDowell, N. G., Fisher, R. A., Wei, L., Sevanto, S., Christoffersen, B. O., et al. (2019). Increasing impacts of extreme droughts on vegetation productivity under climate change. *Nature Climate Change*, *9*(12), 948–953. https://doi.org/10.1038/s41558-019-0630-6

Yin, P., & Fan, X. (2001). Estimating R^2 shrinkage in multiple regression: A comparison of different analytical methods. *The Journal of Experimental Education*, *69*(2), 203–224. https://doi.org/10.1080/00220970109600656

Zeng, Y., Su, Z., Wan, L., & Wen, J. (2011a). Numerical analysis of air-water-heat flow in unsaturated soil: Is it necessary to consider airflow in land surface models? *Journal of Geophysical Research*, *116*(D20), D20107. https://doi.org/10.1029/2011jd015835

Zeng, Y., Su, Z., Wan, L., & Wen, J. (2011b). A simulation analysis of the advective effect on evaporation using a two-phase heat and mass flow model. *Water Resources Research*, *47*(10), W10529. https://doi.org/10.1029/2011wr010701

Zeng, Y., Wan, L., Su, Z., Huang, K., & Wang, X. (2007). *The variation in soil temperature and its effects on the movement of water vapor in the surface zone*. ITC, Twente University.

References From the Supporting Information

Brændholt, A., Steenberg Larsen, K., Ibrom, A., & Pilegaard, K. (2017). Overestimation of closed-chamber soil CO_2 effluxes at low atmospheric turbulence. *Biogeosciences*, *14*(6), 1603–1616. https://doi.org/10.5194/bg-14-1603-2017

Brutsaert, W. (2005). *Hydrology—An introduction*. Cambridge University Press.

Brutsaert, W. (2014b). The daily mean zero-flux plane during soil-controlled evaporation: A Green's function approach. *Water Resources Research*, *50*(12), 9405–9413. https://doi.org/10.1111/j.1752-1688.1969.tb04897.x

Daamen, C. C., Simmonds, L. P., Wallace, J. S., Laryea, K. B., & Sivakumar, M. V. K. (1993). Use of microlysimeters to measure evaporation from sandy soils. *Agricultural and Forest Meteorology*, *65*(3–4), 159–173. https://doi.org/10.1016/0168-1923(93)90002-y

Fayer, M. J., & Simmons, C. S. (1995). Modified soil water retention functions for all matric suctions. *Water Resources Research*, *31*(5), 1233–1238. https://doi.org/10.1029/95wr00173

Haghighi, E., & Kirchner, J. W. (2017). Near-surface turbulence as a missing link in modeling evapotranspiration-soil moisture relationships. *Water Resources Research*, *53*(7), 5320–5344. https://doi.org/10.1002/2016WR020111

Haghighi, E., & Or, D. (2013). Evaporation from porous surfaces into turbulent airflows: Coupling eddy characteristics with pore-scale vapor diffusion. *Water Resources Research*, *49*(12), 8432–8442. https://doi.org/10.1002/2012WR013324

Ho, C. K., & Webb, S. W. (1996). Diffusion mechanisms, models, and data—Does enhanced vapor-phase diffusion exist?

Ho, C. K., & Webb, S. W. (2006). Gas transport in porous media. In J. Bear (Ed.), *Theory and applications of transport in porous media*. Springer. https://doi.org/10.1017/S0022112000211312

Jackson, R. D., Kimball, B. A., Reginato, R. J., & Nakayama, F. S. (1973). Diurnal soil-water evaporation: Time-depth-flux patterns. *Soil Science Society of America Proceedings*, *37*(4), 505–509. https://doi.org/10.2136/sssaj1973.03615995003700040014x

Khalil, M., Sakai, M., Mizoguchi, M., & Miyazaki, T. (2003). Current and prospective applications of Zero Flux Plane (ZFP) method. *Journal of the Japanese Society of Soil Physics*, *95*(3), 75–90.

Khlosi, M., Cornelis, W. M., Douaik, A., van Genuchten, M. T., & Gabriels, D. (2008). Performance evaluation of models that describe the soil water retention curve between saturation and oven dryness. *Vadose Zone Journal*, *7*(1), 87–96. https://doi.org/10.2136/vzj2007.0099

Lu, S., Ren, T., Gong, Y., & Horton, R. (2008). Evaluation of three models that describe soil water retention curves from saturation to oven dryness. *Soil Science Society of America Journal*, *72*(6), 1542–1546. https://doi.org/10.2136/sssaj2007.0307n

Lubczynski, M. W. (2011). Groundwater evapotranspiration: Underestimated role of tree transpiration and bare soil evaporation in groundwater balances of dry lands. In A. Baba, O. Gunduz, M. J. Friedel, G. Tayfur, K. W. F. Howard, & A. Chambel (Eds.), *Climate Change and its Effects on Water Resources: Issues of National and Global Security* (pp. 183–190). Springer. https://link.springer.com/chapter/10.1007/978-94-007-1143-3_21

Millington, R., & Quirk, J. (1960). Permeability of porous solids. *Transactions of the Faraday Society*, *57*, 1200–1207. https://doi.org/10.1039/tf9615701200

Mosthaf, K., Helmig, R., & Or, D. (2014). Modeling and analysis of evaporation processes from porous media on the REV scale. *Water Resources Research*, *50*(2), 1059–1079. https://doi.org/10.1002/2016WR018954

Reyes-Acosta, J. L., & Lubczynski, M. W. (2013). Mapping dry-season tree transpiration of an oak woodland at the catchment scale, using object-attributes derived from satellite imagery and sap flow measurements. *Agricultural and Forest Meteorology*, *174–175*, 184–201. https://doi.org/10.1016/j.agrformet.2013.02.012

Shahraeeni, E., & Or, D. (2012). Pore-scale mechanisms for enhanced vapor transport through partially saturated porous media. *Water Resources Research*, *48*(5), 1–16. https://doi.org/10.1029/2011WR011036

Shokri, N., Lehmann, P., & Or, D. (2009). Critical evaluation of enhancement factors for vapor transport through unsaturated porous media. *Water Resources Research*, *45*(10), 1–9. https://doi.org/10.1029/2009WR007769

Tsujimura, M., Numaguti, A., Tian, L., Hashimoto, S., Sugimoto, A., & Nakawo, M. (2001). Behavior of subsurface water revealed by stable isotope and tensiometric observation in the Tibetan Plateau. *Journal of the Meteorological Society of Japan*, *79*(1B), 599–605. https://doi.org/10.2151/jmsj.79.599

Webb, S. W. (2000). A simple extension of two-phase characteristic curves to include the dry region. *Water Resources Research*, *36*(6), 1425–1430. https://doi.org/10.1029/2000wr900057